ACS APPLIED MATERIALS & INTERFACES

www.acsami.org

Research Article

Quasi-Solid-State Electrolyte Synthesized Using a Thiol−Ene Click Chemistry for Rechargeable Lithium Metal Batteries with Enhanced Safety

Sungguk Park, Bora Jeong, Da-Ae Lim, Chul Haeng Lee, Kyoung Ho Ahn, Jung Hoon Lee, and Dong-Won Kim*

Cite This: *ACS Appl. Mater. Interfaces* 2020, 12, 19553−19562

Read Online

ACCESS | Metrics & More | Article Recommendations | Supporting Information

ABSTRACT: Liquid electrolytes currently used in lithium-ion batteries have critical drawbacks such as high flammability, high reactivity toward electrode materials, and solvent leakage. To overcome these issues, most recent research has focused on synthesis and characterization of highly conductive gel-type polymer electrolytes containing large numbers of organic solvents in the polymer matrix. There are still many hurdles to overcome, however, before they can be applied to commercial-level lithium-ion batteries. Since a large amount of organic solvent is required to achieve high ionic conductivity, battery safety is not significantly enhanced. In our study, we synthesized highly conductive quasi-solid-state electrolytes (QSEs) containing an ionically conductive oligomer (polycaprolactone triacrylate) and a small amount of organic solvent by employing click chemistry. In the QSE, polycaprolactone participates in dissociation of lithium salt and migration of lithium ions, resulting in high ionic conductivity. The Li/$LiNi_{0.6}Co_{0.2}Mn_{0.2}O_2$ cell that used this QSE exhibited good cycling performance and enhanced thermal stability, and durability; no organic solvent leakage was observed even under high pressure.

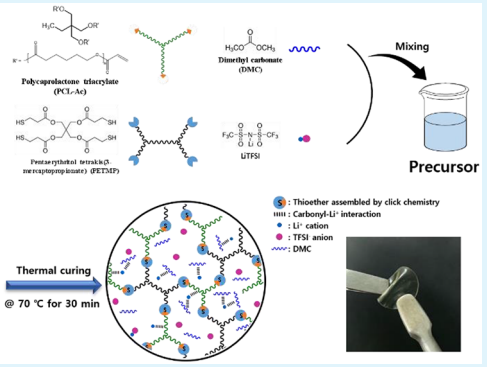

KEYWORDS: *quasi-solid-state electrolyte, click chemistry, polycaprolactone, thermal stability, lithium metal battery*

INTRODUCTION

Demand for high-energy density lithium-ion batteries (LIBs) has been growing rapidly with technological advances in mobile electronic devices, electric vehicles (EVs), and grid-scale energy storage systems (ESSs).[1−3] These LIBs, however, have a critical drawback related to safety. Because they employ a highly flammable liquid electrolyte, abnormal operational conditions can lead to fire or explosions.[4,5] To enhance LIB safety, an effort has been devoted to replacing the liquid electrolyte with a more reliable and safer electrolyte system.[6,7] Various promising electrolyte candidates have been proposed including solid-state electrolytes, ionic liquid-based electrolytes, and gel polymer electrolytes. Solid-state electrolytes offer tremendous battery safety enhancements because the flammable organic solvents are excluded.[8] However, these electrolytes suffer from low ionic conductivity at ambient temperatures and exhibit extremely high interfacial resistance between the solid electrolyte and solid electrodes, leading to poor cycling performance.[9−11] Although ionic liquid-based electrolytes have enhanced thermal and oxidative stability, they have cathodic instability, high viscosity, poor polyolefin separator wettability, and high cost.[12,13] Gel polymer electrolytes are composed of a polymer matrix and large number of organic solvents, offering relatively high ionic conductivity at a reasonable price. Furthermore, chemically cross-linked gel polymer electrolytes can prevent solvent leakage by encapsulating organic solvent in the polymer matrix.[14−17] In spite of these attractive properties, cross-linked gel polymer electrolytes still have challenging issues to overcome. First, gel polymer electrolytes have limited thermal stability because of the large number of organic solvents used to achieve an ionic conductivity exceeding 1 mS cm^{-1}.[18,19] Second, side reactions may occur during the cross-linking reaction when forming the gel. This can cause capacity fading due to impurities affecting electrochemical performance. One of the approaches to solve the above issues is to use a quasi-solid-state electrolyte (QSE), which contains a minimum amount of organic solvents in the solid-state electrolyte. The cell employing QSE exhibited enhanced safety compared with the liquid electrolyte-based cell and better cycling performance than all-solid-state lithium batteries at ambient temperature. That is, the QSE has the

Received: February 12, 2020
Accepted: April 6, 2020
Published: April 6, 2020

combining advantages of liquid (good cycling performance) and solid (enhanced safety) electrolyte. Therefore, many efforts have been focused on the preparation and characterization of QSEs that balance cell performance and safety.[20−23] However, the development of quasi-solid-state lithium batteries still struggles due to the drawbacks including insufficient ionic conductivity, complicated fabrication processes, and low safety level.[24−26]

In our study, highly conductive quasi-solid-state electrolytes were synthesized and applied to a Li/$LiNi_{0.6}Co_{0.2}Mn_{0.2}O_2$ cell. To achieve high ionic conductivity with the QSE, polycaprolactone triacrylate (PCL-Ac) was synthesized and employed as a cross-linking agent as well as a polymer electrolyte. Polycaprolactone can solvate lithium salt and conduct Li^+ ions because it is composed of repeating polar ester units and has high chain flexibility with a glass transition temperature of −66 °C.[27,28] Accordingly, high ionic conductivity can be achieved by incorporating a small amount of organic solvent. To synthesize the chemically cross-linked polymer electrolyte, we used thiol−ene click chemistry, since the click reaction avoids side reactions and drives fast cross-linking under mild reaction conditions.[29−32] The resulting QSE was applied to a lithium metal cell composed of a Li metal anode and a $LiNi_{0.6}Co_{0.2}Mn_{0.2}O_2$ cathode. We investigated their electrochemical performance, thermal stability, and solvent leakage behavior.

EXPERIMENTAL SECTION

Materials. Polycaprolactone triol (PCL-OH, $M_n \sim 900$) was purchased from Sigma-Aldrich and vacuum-dried at 50 °C for 12 h. Trimethylamine (TEA, anhydrous), tetrahydrofuran (THF, anhydrous), dimethyl carbonate (DMC, anhydrous), and acryloyl chloride were purchased from Sigma-Aldrich and used without any treatment. Pentaerythritol tetrakis(3-mercaptopropionate) (PETMP, Sigma-Aldrich) and *tert*-butyl peroxypivalate (t-BPP, Arkema Inc.) were filtered through a 4 Å molecular sieve to remove moisture. Bis(trifluoromethane) sulfonimide lithium salt (LiTFSI) was purchased from Sigma-Aldrich and dried in a vacuum oven at 100 °C for 12 h. Liquid electrolyte of 1.15 M $LiPF_6$ in ethylene carbonate (EC), ethyl methyl carbonate (EMC), and dimethyl carbonate (DEC) (3/5/2 by volume, battery grade) containing 5 wt % fluoroethylene carbonate (FEC) was purchased from PANAX ETEC Co. Ltd.

Synthesis of Polycaprolactone Triacrylate. PCL-OH (20.0 g, 0.0222 mol), TEA (8.09 g, 0.08 mol), and THF (100 mL) were mixed in a 500 mL round-bottom flask using a magnetic stir bar. Acryloyl chloride (7.24 g, 0.08 mol) in 100 mL of THF was added to the solution for 1 h through a syringe pump at 0 °C. The mixed solution was stirred for 48 h at 25 °C under an argon atmosphere. The solution was transferred to a rotary evaporator to remove the THF at 50 °C. The resulting material was diluted with a mixture of distilled water and diethyl ether for extraction. The water was removed, and diethyl ether containing polycaprolactone triacrylate (PCL-Ac) was extracted. The extracted solution was mixed with magnesium sulfate anhydrous (Daejung Chemicals & Metals Co., Ltd.) and stirred with a magnetic bar to remove the remaining water. The magnesium sulfate was filtered-off, and the solution was dried under vacuum at 60 °C to eliminate the diethyl ether. For further purification, the crude product was passed through a chromatography column with 2.0% MeOH in methyl chloroform, yielding pure PCL-Ac.

Electrode Preparation and Cell Assembly. Lithium foil (thickness 100 μm, Honjo Metal Co. Ltd.) was pressed onto a copper current to use as the anode. The cathode was prepared by coating a slurry composed of $LiNi_{0.6}Co_{0.2}Mn_{0.2}O_2$ (Umicore), poly(vinylidiene fluoride) (PVdF, KF7208, Kureha), and super-P carbon with a mass ratio of 95:3:2 in *N*-methyl pyrrolidone (NMP) onto aluminum foil. In the cathode, 12.5 mg cm^{-2} of active $LiNi_{0.6}Co_{0.2}Mn_{0.2}O_2$ material was loaded. The Li/$LiNi_{0.6}Co_{0.2}Mn_{0.2}O_2$ cell was fabricated by stacking the lithium anode, polyethylene (PE) separator (Asahi ND 420), and $LiNi_{0.6}Co_{0.2}Mn_{0.2}O_2$ cathode in a CR2032-type coin cell. The cell was injected with the precursor for QSE, which consisted of click chemistry agents (PCL-Ac, PETMP), LiTFSI, and t-BPP in DMC. The amount of precursor applied to the coin cell was 120 μL. A detailed description of the precursor composition is given in Table 1. The content of DMC in the precursor was maintained at 40 wt %, and a small amount of t-BPP (1.0 wt % with respect to PCL-Ac) was added as an initiator. A water content in the precursor without PETMP was measured to be 21 ppm by Karl Fisher titration using Mettler-Toledo Coulometer. PETMP was excluded when measuring water content, because it can be oxidized by iodine, resulting in erroneously high water content. After cell assembly, the cell was kept at 70 °C for 30 min to induce in situ cross-linking. The Li/$LiNi_{0.6}Co_{0.2}Mn_{0.2}O_2$ cell with PE separator and liquid electrolyte (1.15 M $LiPF_6$ in EC/EMC/DMC (3/5/2 by volume) containing 5 wt % FEC) was also assembled for comparison. The same amount of liquid electrolyte (120 μL) was injected into the cell. The cell assembly was carried out in a glovebox filled with argon gas.

Table 1. Composition of the Precursor Used in Preparation of Quasi-Solid-State Electrolytes

precursor	PCL-Ac (wt %)	PETMP (wt %)	LiTFSI (wt %)	DMC (wt %)
C3S7	13.4	4.6	42.0	40.0
C2S8	8.9	3.1	48.0	40.0
C1S9	4.5	1.5	54.0	40.0

Electrochemical Measurements. For electrochemical measurements, the QSE precursor was injected into a silicon ring in a coin-type cell and thermally cured at 70 °C for 30 min. The ionic conductivity was measured by AC impedance using a CH instrument (CHI 600D) over a frequency range of $10-10^6$ Hz with an amplitude of 50 mV. The electrochemical stability of QSE was evaluated using linear sweep voltammetry (LSV) on a Pt working electrode with lithium metal as the reference and counter electrodes. The scan rate was 1 mV s^{-1} at 25 °C. A cycling test for the Li/$LiNi_{0.6}Co_{0.2}Mn_{0.2}O_2$ cells containing the liquid electrolyte and QSE was performed at a constant current rate in a voltage range of 3.0−4.2 V at 25 °C using a battery test equipment (WBCS 3000, Wonatech).

Characterization. The cross-section of $LiNi_{0.6}Co_{0.2}Mn_{0.2}O_2$ cathode with QSE was obtained using a cross-section polisher (JEOL IB-09020 CP). The cross-sectional morphology of the $LiNi_{0.6}Co_{0.2}Mn_{0.2}O_2$ cathode was examined using field-emission scanning electron microscopy (SEM, JEOL JSM-6330F). Energy dispersive X-ray spectroscopy (EDX) was carried out to investigate the elemental distribution in the cross-sectional area. ^1H NMR spectra of the precursor were recorded in acetone d_6 solvent (Merck KGaA) before and after thermal curing to calculate the conversion of the click reaction. ATR-FTIR spectra were obtained between 400 and 4000 cm^{-1} using a Nicolet iS50 spectrometer. Raman spectroscopy was carried out using a LabRAM HR Evolution Raman spectrometer (Horiba Scientific, 785 nm laser source). The flammability of QSE was investigated by igniting the preweighed electrolyte and measuring the time for the flame to extinguish. The thermal safety of the Li/$LiNi_{0.6}Co_{0.2}Mn_{0.2}O_2$ cell was evaluated by monitoring the open circuit voltage of the charged cell at 150 °C. To investigate the thermal stability of the cathode, we performed DSC measurements of the charged $LiNi_{0.6}Co_{0.2}Mn_{0.2}O_2$ with different electrolytes using differential scanning calorimetry (DSC Q20, TA Instrument) at a heating rate of 10 °C min^{-1} between 50 and 300 °C. The scratched powder containing QSE or liquid electrolyte was used for DSC measurements. We tore two small holes in the pouch bag to investigate the solvent leakage from the quasi-solid-state Li/$LiNi_{0.6}Co_{0.2}Mn_{0.2}O_2$ pouch-type cell. The pouch cell was placed on a flat plate, and a constant 1 kg_f cm^{-2} of pressure was applied to the pouch cell for 30 s. By measuring

https://dx.doi.org/10.1021/acsami.0c02706
ACS Appl. Mater. Interfaces 2020, 12, 19553−19562

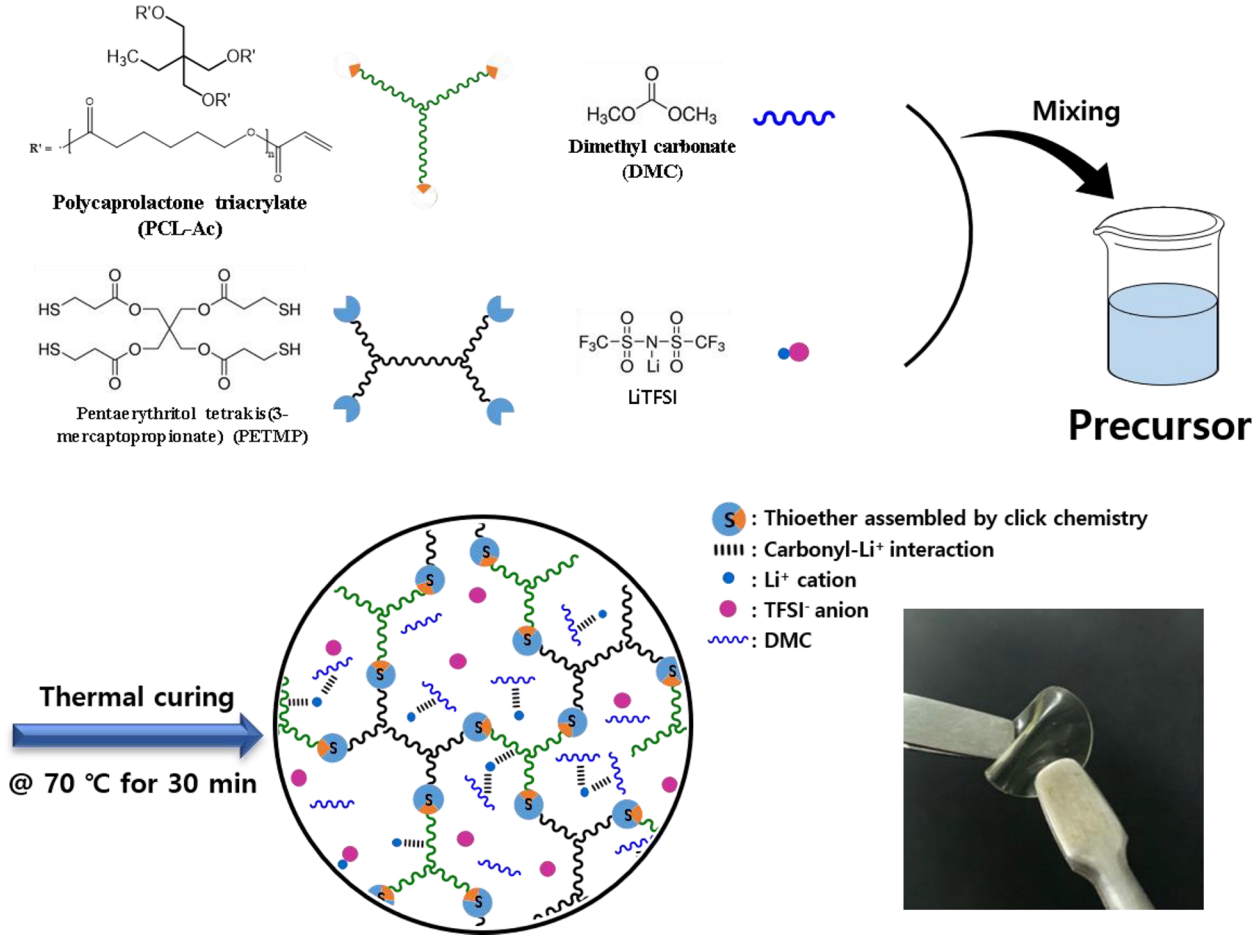

Figure 1. Schematic representation of QSE synthesis by a thiol−ene click chemistry reaction between PETMP (thiol) and PCL-Ac (ene).

the weight of the cell before and after loading, the amount of leakage of solvent was calculated.

RESULTS AND DISCUSSION

Polycaprolactone triacrylate (PCL-Ac) was synthesized from the reaction between polycaprolactone triol (PCL-OH) and acryloyl chloride, as shown in Figure S1. FT-IR spectra of PCL-OH and PCL-Ac are shown in Figure S2. The broad peak observed between 3200 and 3600 cm^{-1} corresponds to the −OH group in PCL-OH. After reacting PCL-OH with acryloyl chloride, the −OH peak disappeared and two new small peaks corresponding with PCL-Ac's vinyl C═C groups appeared at 1400 and 1640 cm^{-1}, respectively. These results indicate successful substitution of −OH groups with acrylate groups. Figure S3a and b show the ^1H NMR spectra of PCL-OH and PCL-Ac, respectively. The peaks observed between 5.8 and 6.5 ppm in Figure S3b are vinyl protons in acrylate, which suggest that PCL-Ac was successfully synthesized from PCL-OH and acryloyl chloride.

Chemically cross-linked QSE was synthesized by a thiol−ene click chemistry reaction between PETMP (thiol) and PCL-Ac (alkene) in the presence of LiTFSI and DMC, as schematically presented in Figure 1. A series of QSEs was obtained by varying the ratio of click chemistry agents (PETMP, PCL-Ac) and salt (3:7, 2:8, 1:9), as previously described in Table 1. The resulting QSEs were free-standing and flexible films with no solvent leakage, irrespective of the precursor composition (Figure 1).

Figure 2a presents the AC impedance spectra of QSEs prepared with C1S9 at different temperatures. Their ionic conductivities were calculated from the electrolyte resistance corresponding to the intercept on the real axis. Figure 2b shows the ionic conductivity for QSEs prepared with different precursors as a function of temperature. As expected, the QSEs' ionic conductivities increased with temperature. With increasing salt content, the ionic conductivity increased and reached a maximum value of 2.2×10^{-3} S cm^{-1} at 25 °C for the QSE prepared with C1S9, which can be ascribed to the increasing number of charge carriers, as salt concentration increased. Linear sweep voltammograms of QSEs at 25 °C are depicted in Figure 2c and d. A small and broad peak observed around 1.0 V vs Li/Li^+ in the cathodic scan is attributed to the reduction of the TFSI anion.[33] The QSEs exhibit a large cathodic current at 0 V vs Li/Li^+, which corresponds to the reductive deposition of lithium onto the working electrode. The anodic scan reveals that all QSEs have oxidative stability exceeding 4.7 V vs Li/Li^+. Among the QSEs investigated, the QSE prepared with C1S9 showed the highest anodic stability. This is attributed to the high salt concentration in the electrolyte, as previously reported.[34−36]

To investigate whether the PCL in QSE participates in lithium salt dissolution, we performed vibrational spectroscopy analysis. Liquid electrolytes and QSEs with different salt concentrations were prepared, as given in Table 2.

FTIR spectra were recorded to investigate the change of local structure of carbonate and ester groups in DMC and

https://dx.doi.org/10.1021/acsami.0c02706
ACS Appl. Mater. Interfaces 2020, 12, 19553−19562

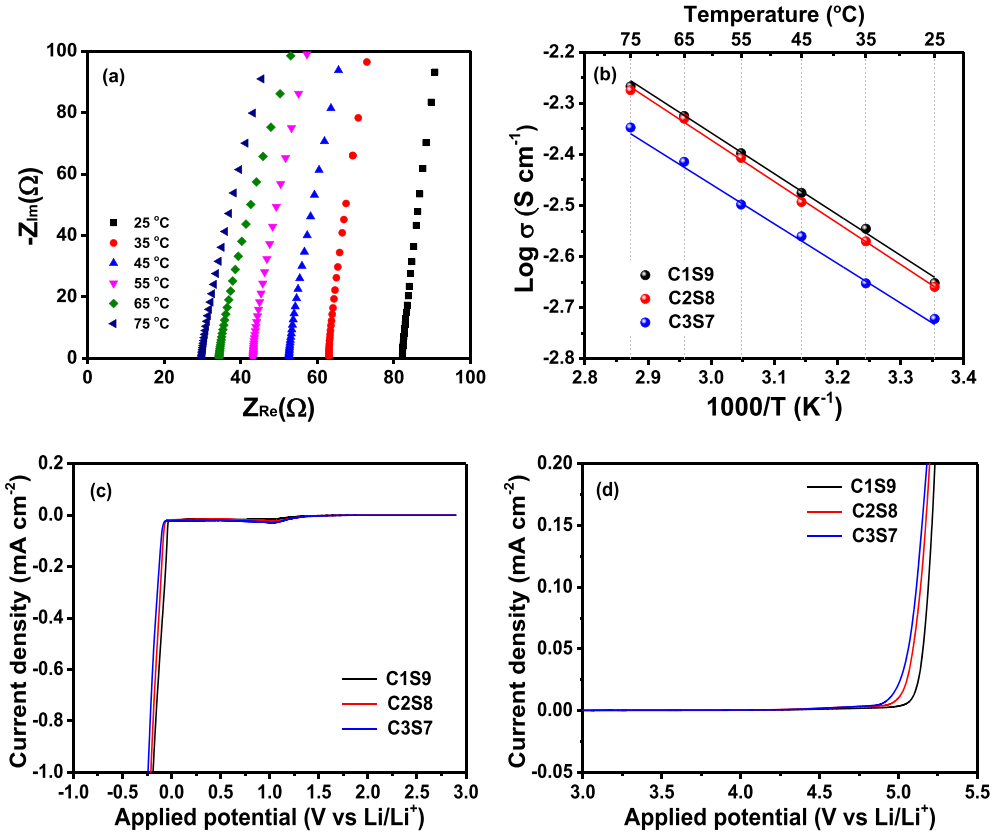

Figure 2. (a) AC impedance spectra of QSE prepared with C1S9 at different temperatures and (b) temperature dependence of ionic conductivity for QSEs with different composition. Linear sweep voltammograms of QSEs at scan rate of 1 mV s^{-1} and 25 °C: (c) cathodic scan and (d) anodic scan.

Table 2. Composition of Liquid Electrolytes and QSEs for Vibrational Spectroscopy Studies

electrolyte		PCL-Ac (g)	PETMP (g)	LiTFSI (g)	DMC (g)
liquid electrolyte	LE 1.5	0	0	1.5	4.0
	LE 3.0	0	0	3.0	4.0
	LE 4.5	0	0	4.5	4.0
	LE 5.4	0	0	5.4	4.0
quasi-solid-state electrolyte	QSE 1.5	0.45	0.15	1.5	4.0
	QSE 3.0	0.45	0.15	3.0	4.0
	QSE 4.5	0.45	0.15	4.5	4.0
	QSE 5.4	0.45	0.15	5.4	4.0

PCL-Ac as a function of salt concentration. Figures 3a and b show the FTIR spectra of liquid electrolytes and QSEs with different salt concentrations. In Figure 3a, the stretching vibration peaks for carbonate C═O and carbonate C═O···Li^+ in the liquid electrolyte were observed at 1751 and 1719 cm^{-1},[37−40] respectively. As salt concentration increased, the proportion of C═O···Li^+ increased from 45.1% (LE 1.5) to 72.4% (LE 5.4), as shown in Table S1. When the QSE peak was deconvoluted, four types of vibrational peaks were observed: carbonate C═O (DMC) at 1751 cm^{-1}, ester C═O (PCL) at 1733 cm^{-1}, carbonate C═O (DMC)···Li^+ at 1719 cm^{-1}, and ester C═O (PCL)···Li^+ at 1706 cm^{-1}[41] (Figure 3b). The relative intensities of carbonate C═O···Li^+ and ester C═O···Li^+ peaks increased with salt concentration (Table S1).

Raman spectroscopy was also performed, and the results are given in Figures 4 and S4. In the Raman spectra of Figures 4a and b, the peaks observed at 743, 746, and 750 cm^{-1} can be assigned to CF_3 bending vibrations of the TFSI anion in the free ions, contact ion pair (CIP), and aggregates (AGG), respectively.[42−45] Figure 4c shows that the relative proportion of free TFSI anions was always higher in the QSEs than in the liquid electrolytes. These results demonstrate that PCL in the QSE participates in lithium salt dissolution. The results of FT-IR and Raman spectroscopy confirmed that PCL-Ac not only plays a role as a cross-linking agent for click chemistry reactions but also dissolves lithium salt and thus creates more free ions. Such a characteristic of PCL-Ac leads to high ionic conductivity of QSE (2.2×10^{-3} S cm^{-1} at 25 °C) even with a low DMC content. The electrochemical characteristics of liquid electrolyte (LE 5.4) and QSE (QSE 5.4) are compared in Figure S5. Although the QSE exhibited lower ionic conductivity than the liquid electrolyte, the oxidative stability of the QSE was much higher than that of the liquid electrolyte. This result suggests that the thermal cross-linking through the click reaction contributes to the enhancement of the electrochemical stability.

Minimizing any unreacted reactants in the QSEs after the cross-linking reaction is necessary, so we calculated conversion of reactants in the click chemistry reaction using ^{1}H NMR analysis. For comparison, we also measured the conversion of reactants in the conventional free-radical reactions. The precursor for the click chemistry reaction was C1S9 (Table 1), while the precursor for the radical reaction was PCL-Ac and t-BPP without PETMP. A small amount (0.5 wt %) of

https://dx.doi.org/10.1021/acsami.0c02706
ACS Appl. Mater. Interfaces 2020, 12, 19553−19562

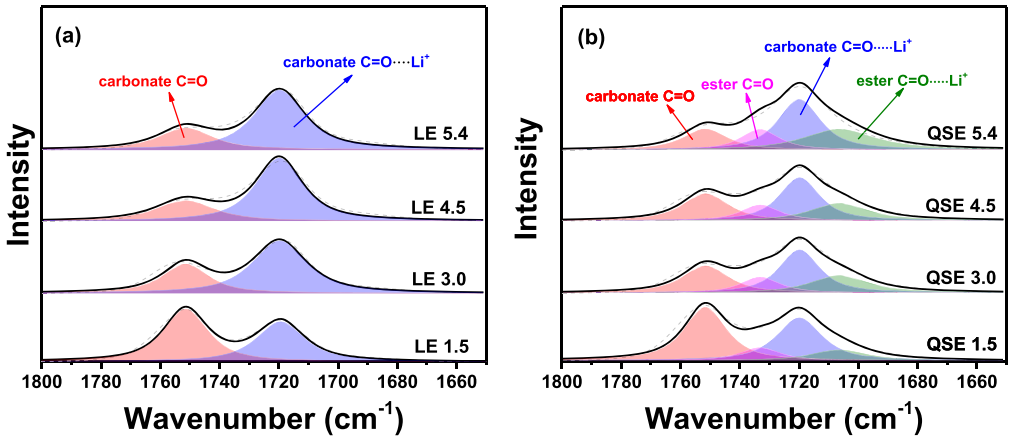

Figure 3. FT-IR spectra of (a) liquid electrolytes and (b) QSEs with different salt concentrations.

ethylene carbonate (EC) was intentionally added to these precursors as an internal standard. Before thermal curing, the precursors containing EC were dissolved in acetone-d_6 and subjected to ^{1}H NMR analysis. In the ^{1}H NMR spectra of the precursors in Figure 5, the peaks observed at 6.35, 6.13, and 5.82 ppm can be assigned to protons (B), (C), and (D) of acrylate in PCL-Ac. The large and sharp peak at 4.54 ppm corresponds to proton (A) of EC. Its integrated intensity was used as a reference value for calculating the relative intensities of acrylate's protons (B), (C), and (D). The intensities of protons (B), (C), and (D) with respect to proton (A) before curing are denominated as I_0^b, I_0^c, and I_0^d, respectively. The precursors were thermally cured at 70 °C for 30 min, and the resulting QSEs were mixed with acetone-d_6 to extract EC and unreacted reactants. The extracted solutions were transferred into NMR tubes for ^{1}H NMR analysis. In the same way as above, the intensity of protons (B), (C), and (D) in unreacted acrylate compared to proton (A) in EC after curing are expressed as I_f^b, I_f^c, and I_f^d, respectively. The reaction conversion of QSE could be then calculated by eq 1:

$$\text{conversion}\ (\%) = \left(1 - \frac{1}{3}\left(\frac{I_f^b}{I_0^b} + \frac{I_f^c}{I_0^c} + \frac{I_f^d}{I_0^d}\right)\right) \times 100 \quad (1)$$

Comparison of the ^{1}H NMR spectra of two QSEs (Figure 5c and d) reveals that the relative intensities of protons (B), (C), and (D) in QSE obtained by click chemistry reaction are much smaller than those in QSE obtained by radical polymerization. Reaction conversions, calculated using eq 1, were 96.8% and 88.0% for the click chemistry and radical reactions, respectively. This result implies that thermal curing by click chemistry reaction proceeds more rapidly than radical polymerization. Thus, the click reaction can attain higher conversion or higher degree of cross-linking compared to the radical reaction in a shorter time (30 min). These results demonstrate that the unreacted residual reactants can be minimized by synthesizing QSE through a click chemistry reaction rather than through radical polymerization.

Before cell assembly, the cross-sectional FE-SEM and EDX mapping images were obtained to confirm whether the QSEs deeply penetrated the pores of the electrodes. We spread the C1S9 precursor onto the $LiNi_{0.6}Co_{0.2}Mn_{0.2}O_2$ cathode, and it was thermally cured at 70 °C for 30 min. The resulting cross-sectional FE-SEM and EDX mapping images are presented in Figure 6. As shown in Figure 6a, the precursor had penetrated into the electrode and was fully cross-linked. Some holes observed in the SEM image are attributed to DMC evaporation under vacuum during cross-sectional polishing and FE-SEM measurements. The EDX mapping image of sulfur arising from PETMP and LiTFSI in Figure 6b demonstrates that QSEs are deeply embedded and uniformly distributed within the $LiNi_{0.6}Co_{0.2}Mn_{0.2}O_2$ electrode. These results demonstrate that the continuous conduction pathways of lithium ions are well formed by QSE in the electrode.

The Li/$LiNi_{0.6}Co_{0.2}Mn_{0.2}O_2$ cell was assembled with QSE made using the C1S9 precursor. Before the cycling test, the cell was preconditioned by cycling in the voltage range of 3.0 to 4.2 V at 0.05 C rate for two cycles and then charge−discharge cycled at a rate of 0.2 C at 25 °C. The voltage profiles and cycling performance of the QSE Li/$LiNi_{0.6}Co_{0.2}Mn_{0.2}O_2$ cell after the preconditioning cycles are shown in Figure 7a and b, respectively. The cell initially delivered a discharge capacity of 146.8 mAh g^{-1} based on the mass of $LiNi_{0.6}Co_{0.2}Mn_{0.2}O_2$ material in the cathode. During the repeated testing, the cell exhibited good stability with Coulombic efficiencies higher than 99.5% throughout. After 100 cycles, it delivered a discharge capacity of 142.2 mAh g^{-1}, which corresponds to 96.9% of its initial discharge capacity. For comparison, the Li/$LiNi_{0.6}Co_{0.2}Mn_{0.2}O_2$ cell with liquid electrolyte was cycled under the same conditions. Its cycling performance is presented in Figure S6. Although its initial discharge capacity (~150.6 mAh g^{-1}) was somewhat higher than that of the cell with QSE, the capacity retention (93.2%) was lower. This result suggests that replacing the liquid electrolyte with QSE could improve the cycling stability of the Li/$LiNi_{0.6}Co_{0.2}Mn_{0.2}O_2$ cell.

To investigate the interfacial stability, AC impedance spectra of the Li/$LiNi_{0.6}Co_{0.2}Mn_{0.2}O_2$ cells with different electrolytes were obtained before and after 100 cycles, and the results are presented in Figure S7. In these spectra, the left semicircle is associated with resistance of solid electrolyte interphase (SEI) formed on the Li electrode (R_{SEI}), and the right one is attributed to the charge transfer resistance at electrode−electrolyte interface (R_{ct}), as given in the equivalent circuit. In the cell with liquid electrolyte, R_{SEI} was remarkably increased after cycling, which can be ascribed to the growth of the resistive layer on the Li electrode due to the deleterious reaction with liquid electrolyte. In contrast, the increase of cell resistances (R_e, R_{SEI}, R_{ct}) in the cell employing QSE was not so significant as compared to those of the liquid electrolyte-based

https://dx.doi.org/10.1021/acsami.0c02706
ACS Appl. Mater. Interfaces 2020, 12, 19553−19562

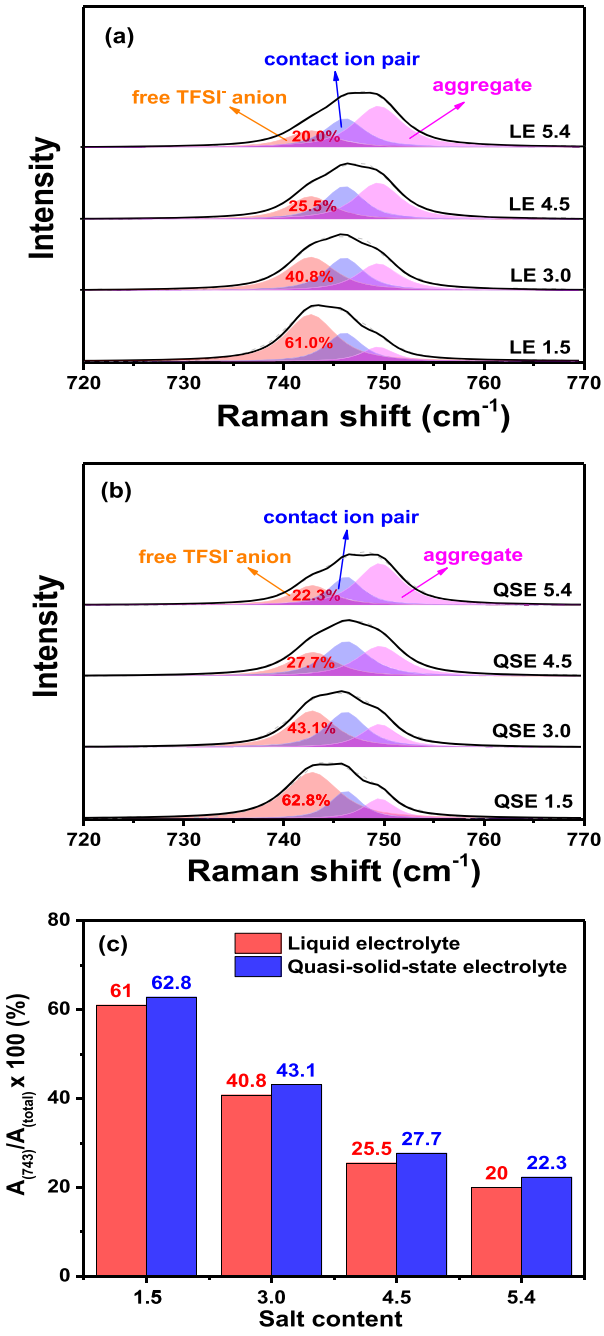

Figure 4. Raman spectra of (a) liquid electrolytes and (b) QSEs with different lithium salt concentrations. (c) Degree of salt dissociation in liquid electrolytes and QSEs with different salt content.

cell. These results suggest that the use of QSE in the Li/$LiNi_{0.6}Co_{0.2}Mn_{0.2}O_2$ cell can improve the cycling stability. The Li/$LiNi_{0.6}Co_{0.2}Mn_{0.2}O_2$ cells were disassembled after 100 cycles and the morphologies of lithium electrodes were examined using scanning electron microscope. As shown in Figure S8a, the lithium electrode cycled in the liquid electrolyte exhibited a dendritic morphology with highly rough and uneven surface, which was caused by irregular lithium ion flux and side reactions between liquid electrolyte and lithium electrode. In contrast, the lithium electrode cycled with QSE showed a relatively flat and smooth surface (Figure S8b). This is because that the use of QSE allows the uniform lithium ion flux through the electrolyte and good interfacial contact between QSE and lithium electrode. These results suggest that QSE leads to the uniform deposition and stripping of lithium during cycling, resulting in enhancement of the cycling stability of the Li/$LiNi_{0.6}Co_{0.2}Mn_{0.2}O_2$ cell.

We also evaluated the rate capability of the quasi-solid-state Li/$LiNi_{0.6}Co_{0.2}Mn_{0.2}O_2$ cell. The cell was charged to 4.2 V at a rate of 0.1 C and discharged to 3.0 V at different current rates. This cycle was repeated five times at each C rate. The first discharge curves of the quasi-solid-state Li/$LiNi_{0.6}Co_{0.2}Mn_{0.2}O_2$ cell obtained at each current rate are presented in Figure 8a. As the current rate increased, the overpotential gradually increased and the discharge capacity decreased. As a result, the cell delivered a reduced discharge capacity of 111.9 mAh g^{-1} at the 1.0 C rate. Figure 8b compares the discharge capacities of the cells assembled with liquid electrolyte and QSE. The quasi-solid-state Li/$LiNi_{0.6}Co_{0.2}Mn_{0.2}O_2$ cell delivered lower discharge capacities than the cell with liquid electrolyte at all the current rates. This can be ascribed to the higher internal cell resistance of the quasi-solid-state cell. The quasi-solid-state Li/$LiNi_{0.6}Co_{0.2}Mn_{0.2}O_2$ cell recovered a reversible capacity at the 0.1 C rate after cycling at high current rates, indicating its good cycling stability.

The flammabilities of liquid electrolyte (1.15 M $LiPF_6$ in EC/EMC/DMC) and QSE prepared with C1S9 were compared. Figure S9 presents the photographs of liquid electrolyte and QSE during the flammability test. When liquid electrolyte was exposed to a flame source, it caught a fire immediately and was burned for a long time. Its self-extinguishing time (SET) was measured to be 228.5 s g^{-1}. In contrast, QSE burned during ignition with a flame source, but extinguished immediately after removing the flame source. Its SET value was 1.2 s g^{-1}. These results imply that QSE is an almost nonflammable electrolyte.

To compare the thermal stability of the cells assembled with liquid electrolyte and quasi-solid-state electrolyte, the Li/$LiNi_{0.6}Co_{0.2}Mn_{0.2}O_2$ cells were fully charged to 4.2 V. The cells were disassembled in an argon-filled glovebox, and the charged $Li_{1-x}Ni_{0.6}Co_{0.2}Mn_{0.2}O_2$ material with electrolyte was collected by scratching it from the current collector. DSC measurements were then performed, and the resulting thermograms are shown in Figure 9. As shown in the figure, the delithiated $Li_{1-x}Ni_{0.6}Co_{0.2}Mn_{0.2}O_2$ material with liquid electrolyte showed large exothermic peaks around 248.2 °C with an exothermic heat of 520.0 J g^{-1}. This is due to the exothermic reaction between $Li_{1-x}Ni_{0.6}Co_{0.2}Mn_{0.2}O_2$ and the liquid electrolyte. In contrast, the charged $Li_{1-x}Ni_{0.6}Co_{0.2}Mn_{0.2}O_2$ material with quasi-solid-state electrolyte exhibited a small exothermic peak at 272.7 °C with a heat flow of 135.9 J g^{-1}. These results demonstrate that QSE is less reactive toward the delithiated $Li_{1-x}Ni_{0.6}Co_{0.2}Mn_{0.2}O_2$ cathode material, which results in higher peak temperatures and reduced exothermic heat, which can lead to enhanced thermal stability for the quasi-solid-state Li/$LiNi_{0.6}Co_{0.2}Mn_{0.2}O_2$ cell.

The thermal safety of Li/$LiNi_{0.6}Co_{0.2}Mn_{0.2}O_2$ cells assembled with liquid electrolyte and QSE was compared by recording the voltage of the charged cells at 150 °C for 1 h, and the results are presented in Figure S10. The voltage of the cell with liquid electrolyte dropped to 0 V due to the short-circuit caused by thermal shrinkage of PE separator at high temperature. On the other hand, the voltage of the cell employing QSE was slightly decreased to 3.75 V without sudden voltage drop during heat exposure at 150 °C. These

https://dx.doi.org/10.1021/acsami.0c02706
ACS Appl. Mater. Interfaces 2020, 12, 19553−19562

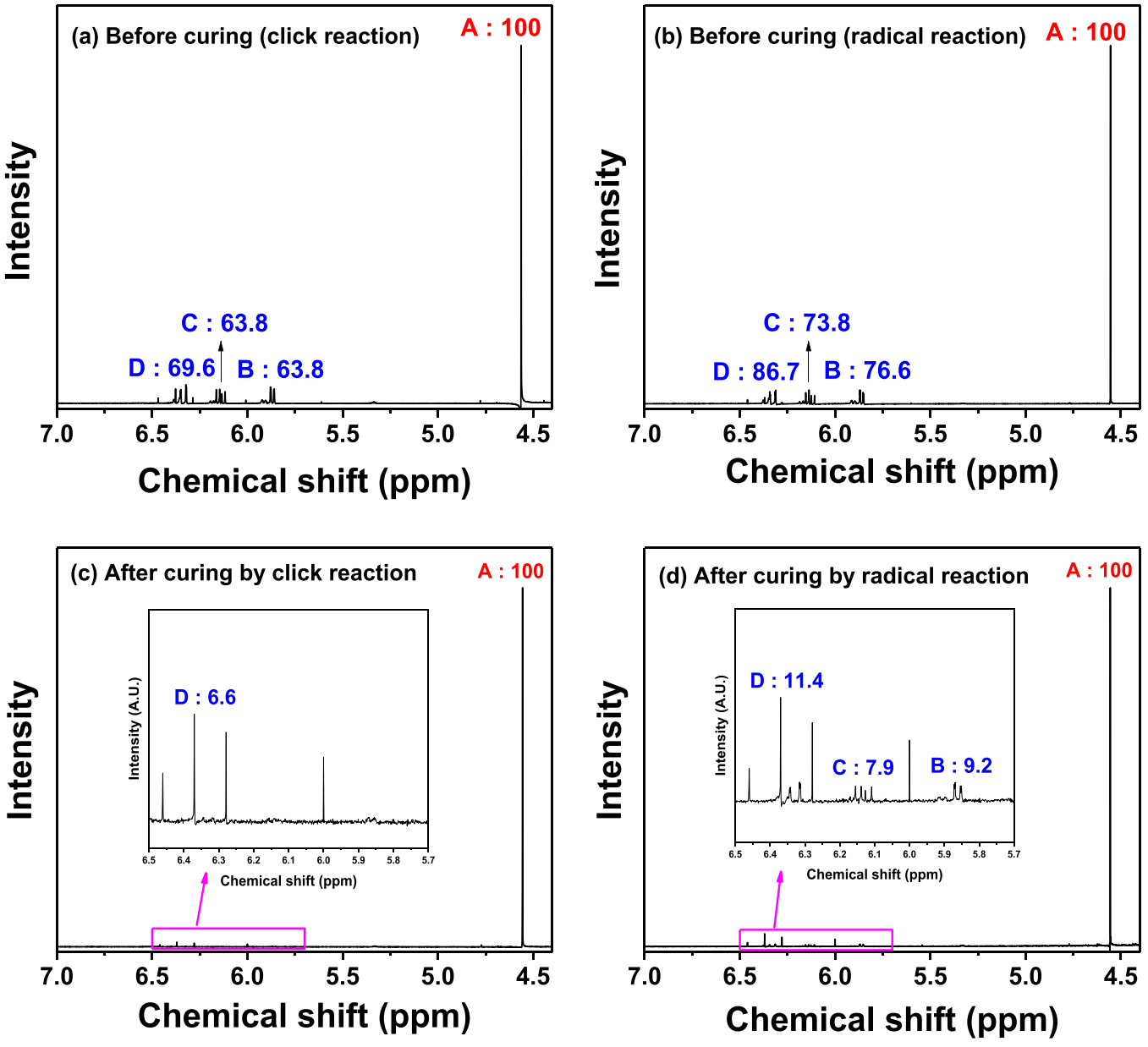

Figure 5. ^{1}H NMR spectra of precursors before (a) click chemistry and (b) radical reactions and ^{1}H NMR spectra of the QSE extracted samples obtained by (c) click chemistry and (d) radical reactions.

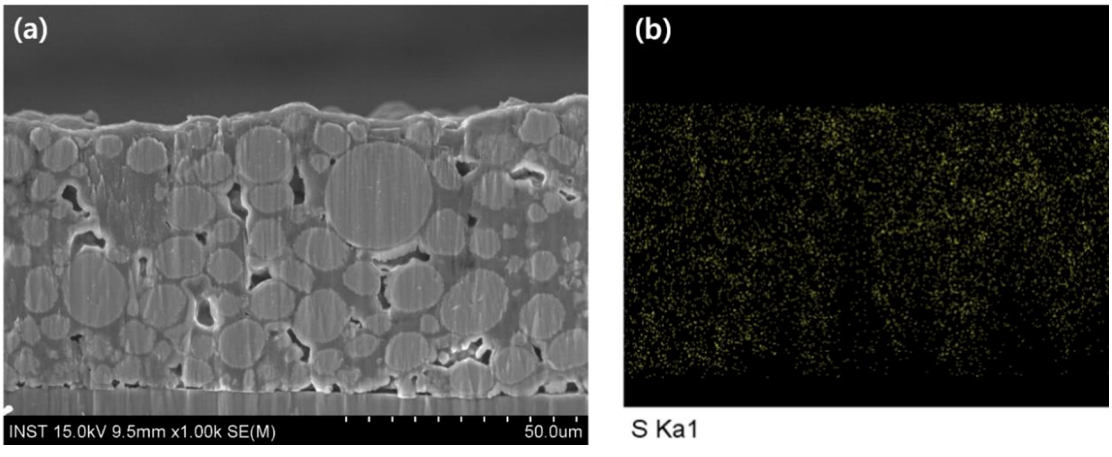

Figure 6. (a) Cross-sectional SEM and (b) EDX mapping images of the $LiNi_{0.6}Co_{0.2}Mn_{0.2}O_2$ electrode with QSE prepared from C1S9 precursor.

https://dx.doi.org/10.1021/acsami.0c02706
ACS Appl. Mater. Interfaces 2020, 12, 19553−19562

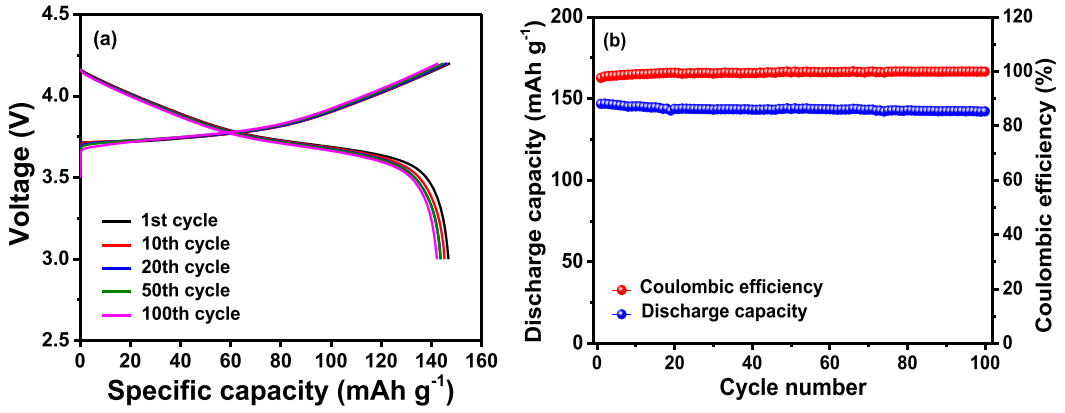

Figure 7. Cycling performance of the quasi-solid-state Li/$LiNi_{0.6}Co_{0.2}Mn_{0.2}O_2$ cell assembled with QSE synthesized from C1S9 at 25 °C. (a) Voltage profiles and (b) discharge capacities as a function of cycle number.

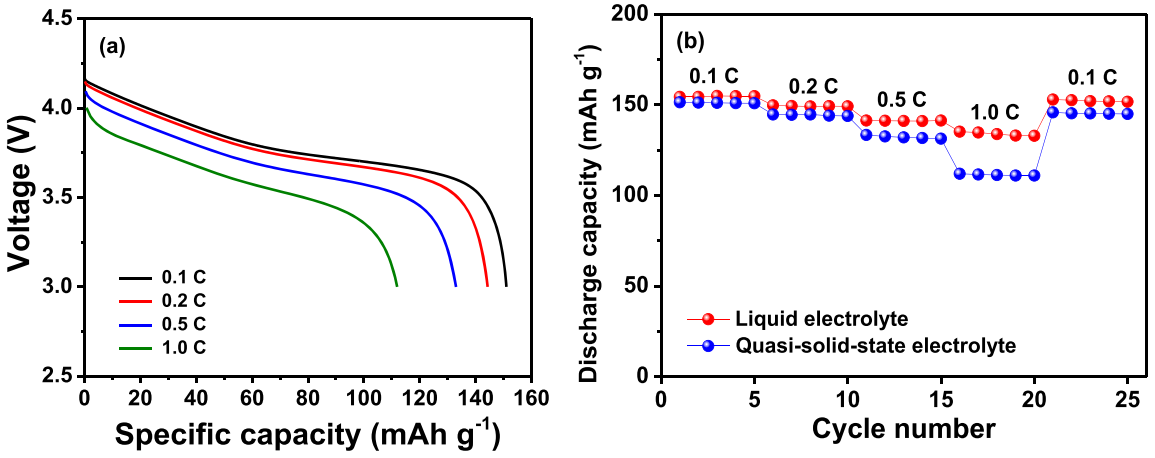

Figure 8. (a) Discharge curves of the quasi-solid-state Li/$LiNi_{0.6}Co_{0.2}Mn_{0.2}O_2$ cell with C1S9 at different current rates and (b) discharge capacities of the cells with different electrolytes as a function of C rate.

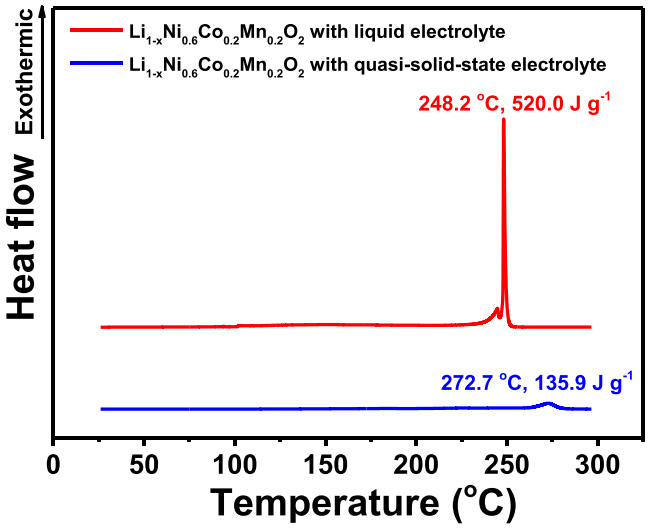

Figure 9. DSC thermograms of the delithiated $Li_{1-x}Ni_{0.6}Co_{0.2}Mn_{0.2}O_2$ materials with liquid electrolyte and QSE.

result indicate that the three-dimensional polymer network formed in QSE prevents the short-circuit at high temperature and thus enhances the thermal safety of the cell.

Leakage of the organic solvent from the cell was also investigated. Figure S11 illustrates the process for testing solvent leakage from the pouch cells. First, a stacked Li/$LiNi_{0.6}Co_{0.2}Mn_{0.2}O_2$ cell with a 120 mAh capacity was fabricated in a pouch bag. Second, two small holes were torn at the top of the pouch bag. The pouch cell was then placed on a flat plate, and a constant pressure of 1 kg_f cm^{-2} was applied to the cell for 30 s. After wiping off the electrolyte leakage with paper, the amount of leakage was calculated by measuring the weight of the pouch cell before and after loading. The quasi-solid-state cell exhibited no leakage. In contrast, the cell assembled with the liquid electrolyte lost 12.8 wt % of its initial amount. These results suggest that the organic solution is effectively encapsulated in the QSE quasi-solid-state cell, which can suppress performance degradation and reduce safety issues associated with flammable organic solvent leakage.

CONCLUSIONS

To enhance battery safety, a quasi-solid-state electrolyte was synthesized using a thiol−ene click chemistry reaction with a precursor consisting of PCL-Ac, PETMP, LiTFSI, and DMC. The resulting QSE exhibited a high ionic conductivity of 2.2×10^{-3} S cm^{-1} and anodic stability exceeding 4.7 V vs Li/Li^+ at ambient temperature. The PCL-Ac used as a cross-linking agent dissolved the lithium salt, leading to a QSE with high ionic conductivity. The thermal curing in the click chemistry reaction was more facile than that through radical polymerization, and the residual reactants could be minimized in the

https://dx.doi.org/10.1021/acsami.0c02706
ACS Appl. Mater. Interfaces 2020, 12, 19553−19562

click reaction. The quasi-solid-state Li/$LiNi_{0.6}Co_{0.2}Mn_{0.2}O_2$ cell assembled with QSE exhibited stable cycling performance and enhanced thermal safety. Our results demonstrate that the QSE synthesized using click chemistry is a safer and more reliable electrolyte system for next-generation lithium metal batteries.

■ ASSOCIATED CONTENT

Supporting Information

The Supporting Information is available free of charge at https://pubs.acs.org/doi/10.1021/acsami.0c02706.

Schematic of the synthesis of PCL-Ac; FT-IR spectra of PCL-OH and PCL-Ac; ^{1}H NMR spectra of PCL-OH and PCL-Ac; relative intensities of carbonyl groups in different electrolytes; Raman spectra of liquid and quasi-solid-state electrolytes with different salt content; ionic conductivity and linear sweep voltammograms of liquid electrolyte and QSE; cycling performance of the Li/$LiNi_{0.6}Co_{0.2}Mn_{0.2}O_2$ cell with liquid electrolyte; AC impedance spectra of the Li/$LiNi_{0.6}Co_{0.2}Mn_{0.2}O_2$ cells; SEM images of lithium electrodes disassembled from the Li/$LiNi_{0.6}Co_{0.2}Mn_{0.2}O_2$ cells; photographs of liquid electrolyte and QSE during flammability test; variation of open circuit voltage of the charged Li/$LiNi_{0.6}Co_{0.2}Mn_{0.2}O_2$ cells at 150 °C; leakage test of the pouch cell (PDF)

■ AUTHOR INFORMATION

Corresponding Author

Dong-Won Kim − *Department of Chemical Engineering and Institute of Nano Science and Technology, Hanyang University, Seoul 04763, Republic of Korea;* orcid.org/0000-0002-1735-0272; Phone: +82 2 2220 2337; Email: dongwonkim@hanyang.ac.kr; Fax: +82 2 2298 4101

Authors

Sungguk Park − *Department of Chemical Engineering, Hanyang University, Seoul 04763, Republic of Korea*

Bora Jeong − *Department of Chemical Engineering, Hanyang University, Seoul 04763, Republic of Korea*

Da-Ae Lim − *Department of Chemical Engineering, Hanyang University, Seoul 04763, Republic of Korea*

Chul Haeng Lee − *Battery R&D, LG Chem, Daejeon 34122, Republic of Korea*

Kyoung Ho Ahn − *Battery R&D, LG Chem, Daejeon 34122, Republic of Korea*

Jung Hoon Lee − *Battery R&D, LG Chem, Daejeon 34122, Republic of Korea*

Complete contact information is available at: https://pubs.acs.org/10.1021/acsami.0c02706

Notes

The authors declare no competing financial interest.

■ ACKNOWLEDGMENTS

The authors would like to thank LG Chem for providing financial support.

■ REFERENCES

(1) Etacheri, V.; Marom, R.; Elazari, R.; Salitra, G.; Aurbach, D. Challenges in the Development of Advanced Li-Ion Batteries: A Review. *Energy Environ. Sci.* **2011**, *4*, 3243−3262.

(2) Goodenough, J. B.; Park, K.-S. The Li-Ion Rechargeable Battery: A Perspective. *J. Am. Chem. Soc.* **2013**, *135*, 1167−1176.

(3) Larcher, D.; Tarascon, J. M. Towards Greener and More Sustainable Batteries for Electrical Energy Storage. *Nat. Chem.* **2015**, *7*, 19−29.

(4) Wang, Q.; Ping, P.; Zhao, X.; Chu, G.; Sun, J.; Chen, C. Thermal Runaway Caused Fire and Explosion of Lithium Ion Battery. *J. Power Sources* **2012**, *208*, 210−224.

(5) Feng, X.; Zheng, S.; He, X.; Wang, L.; Wang, Y.; Ren, D.; Ouyang, M. Time Sequence Map for Interpreting the Thermal Runaway Mechanism of Lithium-Ion Batteries With $LiNi_xCo_yMn_zO_2$ Cathode. *Front. Energy Res.* **2018**, *6*, 126.

(6) Kalhoff, J.; Eshetu, G. G.; Bresser, D.; Passerini, S. Safer Electrolytes for Lithium-Ion Batteries: State of the Art and Perspectives. *ChemSusChem* **2015**, *8*, 2154−2175.

(7) Wang, Q.; Jiang, L.; Yu, Y.; Sun, J. Progress of Enhancing the Safety of Lithium Ion Battery from the Electrolyte Aspect. *Nano Energy* **2019**, *55*, 93−114.

(8) Meesala, Y.; Jena, A.; Chang, H.; Liu, R.-S. Recent Advancements in Li-Ion Conductors for All-Solid-State Li-Ion Batteries. *ACS Energy Lett.* **2017**, *2*, 2734−2751.

(9) Meyer, W. H. Polymer Electrolytes for Lithium-Ion Batteries. *Adv. Mater.* **1998**, *10*, 439−448.

(10) Janek, J.; Zeier, W. G. A Solid Future for Battery Development. *Nature Energy* **2016**, *1*, 16141.

(11) Pervez, S. A.; Cambaz, M. A.; Thangadurai, V.; Fichtner, M. Interface in Solid-State Lithium Battery: Challenges, Progress, and Outlook. *ACS Appl. Mater. Interfaces* **2019**, *11*, 22029−22050.

(12) Armand, M.; Endres, F.; MacFarlane, D. R.; Ohno, H.; Scrosati, B. Ionic-Liquid Materials for the Electrochemical Challenges of the Future. *Nat. Mater.* **2009**, *8*, 621−629.

(13) Wu, F.; Zhu, N.; Bai, Y.; Liu, L.; Zhou, H.; Wu, C. Highly Safe Ionic Liquid Electrolytes for Sodium-Ion Battery: Wide Electrochemical Window and Good Thermal Stability. *ACS Appl. Mater. Interfaces* **2016**, *8*, 21381−21386.

(14) Shin, W.-K.; Yoo, J. H.; Choi, W.; Chung, K. Y.; Jang, S. S.; Kim, D.-W. Cycling Performance of Lithium-Ion Polymer Cells Assembled with Cross-Linked Composite Polymer Electrolyte Using Fibrous Polyacrylonitrile Membrane and Vinyl-Functionalized SiO_2 Nanoparticles. *J. Mater. Chem. A* **2015**, *3*, 12163−12170.

(15) Cui, Y.; Chai, J.; Du, H.; Duan, Y.; Xie, G.; Liu, Z.; Cui, G. Facile and Reliable in Situ Polymerization of Poly(Ethyl Cyanoacrylate)-Based Polymer Electrolytes toward Flexible Lithium Batteries. *ACS Appl. Mater. Interfaces* **2017**, *9*, 8737−8741.

(16) Woo, H.-S.; Moon, Y.-B.; Seo, S.; Lee, H.-T.; Kim, D.-W. Semi-Interpenetrating Polymer Network Composite Gel Electrolytes Employing Vinyl-Functionalized Silica for Lithium-Oxygen Batteries with Enhanced Cycling Stability. *ACS Appl. Mater. Interfaces* **2018**, *10*, 687−695.

(17) Baik, J.-H.; Kim, S.; Hong, D. G.; Lee, J.-C. Gel Polymer Electrolytes Based on Polymerizable Lithium Salt and Poly(ethylene glycol) for Lithium Battery Applications. *ACS Appl. Mater. Interfaces* **2019**, *11*, 29718−29724.

(18) Lee, Y.-W.; Shin, W.-K.; Kim, D.-W. Cycling Performance of Lithium-Ion Polymer Batteries Assembled Using In-Situ Chemical Cross-Linking without a Free Radical Initiator. *Solid State Ionics* **2014**, *255*, 6−12.

(19) Wu, H.; Cao, Y.; Su, H.; Wang, C. Tough Gel Electrolyte Using Double Polymer Network Design for the Safe, Stable Cycling of Lithium Metal Anode. *Angew. Chem., Int. Ed.* **2018**, *57*, 1361−1365.

(20) Judez, X.; Martinez-Ibanez, M.; Santiago, A.; Armand, M.; Zhang, H.; Li, C. Quasi-Solid-State Electrolytes for Lithium Sulfur Batteries: Advances and Perspectives. *J. Power Sources* **2019**, *438*, 226985.

(21) Sun, Q.; Chen, X.; Xie, J.; Xu, X.; Tu, J.; Zhang, P.; Zhao, X. Nonflammable Quasi-Solid-State Electrolyte for Stable Lithium-Metal Batteries. *RSC Adv.* **2019**, *9*, 42183−42193.

(22) Zhong, Y.; Zhong, L.; Wang, S.; Qin, J.; Han, D.; Ren, S.; Xiao, M.; Sun, L.; Meng, Y. Ultrahigh Li-Ion Conductive Single-Ion

Polymer Electrolyte Containing Fluorinated Polysulfonamide for Quasi-Solid-State Li-Ion Batteries. *J. Mater. Chem. A* **2019**, *7*, 24251−24261.
(23) Tan, R.; Gao, R.; Zhao, Y.; Zhang, M.; Xu, J.; Yang, J.; Pan, F. Novel Organic-Inorganic Hybrid Electrolyte to Enable $LiFePO_4$ Quasi-Solid-State Li-Ion Batteries Performed Highly Around Room Temperature. *ACS Appl. Mater. Interfaces* **2016**, *8*, 31273−31280.
(24) Shim, J.; Kim, H. J.; Kim, B. G.; Kim, Y. S.; Kim, D. G.; Lee, J. C. 2D Boron Nitride Nanoflakes as a Multifunctional Additive in Gel Polymer Electrolytes for Safe, Long Cycle Life and High Rate Lithium Metal Batteries. *Energy Environ. Sci.* **2017**, *10*, 1911−1916.
(25) Guo, J. Z.; Yang, A. B.; Gu, Z. Y.; Wu, X. L.; Pang, W. L.; Ning, Q. L.; Li, W. H.; Zhang, J. P.; Su, Z. M. Quasi-Solid-State Sodium-Ion Full Battery with High-Power/Energy Densities. *ACS Appl. Mater. Interfaces* **2018**, *10*, 17903−17910.
(26) Zhou, J.; Ji, H.; Liu, J.; Qian, T.; Yan, C. A New High Ionic Conductive Gel Polymer Electrolyte Enables Highly Stable Quasi-Solid-State Lithium Sulfur Battery. *Energy Storage Mater.* **2019**, *22*, 256−264.
(27) Bergfelt, A.; Lacey, M. J.; Hedman, J.; Sangeland, C.; Brandell, D.; Bowden, T. ε-Caprolactone-Based Solid Polymer Electrolytes for Lithium-Ion Batteries: Synthesis, Electrochemical Characterization and Mechanical Stabilization by Block Copolymerization. *RSC Adv.* **2018**, *8*, 16716−16725.
(28) Eriksson, T.; Mindemark, J.; Yue, M.; Brandell, D. Effects of Nanoparticle Addition to Poly(ε-caprolactone) Electrolytes: Crystallinity, Conductivity and Ambient Temperature Battery Cycling. *Electrochim. Acta* **2019**, *300*, 489−496.
(29) Nair, D. P.; Podgorski, M.; Chatani, S.; Gong, T.; Xi, W.; Fenoli, C. R.; Bowman, C. N. The Thiol-Michael Addition Click Reaction: A Powerful and Widely Used Tool in Materials Chemistry. *Chem. Mater.* **2014**, *26*, 724−744.
(30) Kolb, H. C.; Finn, M. G.; Sharpless, K. B. Click Chemistry: Diverse Chemical Function from a Few Good Reactions. *Angew. Chem., Int. Ed.* **2001**, *40*, 2004−2021.
(31) Hoyle, C. E.; Bowman, C. N. Thiol−Ene Click Chemistry. *Angew. Chem., Int. Ed.* **2010**, *49*, 1540−1573.
(32) Hoyle, C. E.; Lee, T. Y.; Roper, T. Thiol−Enes: Chemistry of the Past with Promise for the Future. *J. Polym. Sci., Part A: Polym. Chem.* **2004**, *42*, 5301−5338.
(33) Gu, Y.; Wang, W.-W.; He, J.-W.; Tang, S.; Xu, H.-Y.; Yan, J.-W.; Wu, Q.-H.; Lian, X.-B.; Zheng, M.-S.; Dong, Q.-F.; Mao, B.-W. Electrochemical Polishing of Lithium Metal Surface for Highly Demanding Solid-Electrolyte Interphase. *ChemElectroChem* **2019**, *6*, 181−188.
(34) Yoshida, K.; Nakamura, M.; Kazue, Y.; Tachikawa, N.; Tsuzuki, S.; Seki, S.; Dokko, K.; Watanabe, M. Oxidative-Stability Enhancement and Charge Transport Mechanism in Glyme-Lithium Salt Equimolar Complexes. *J. Am. Chem. Soc.* **2011**, *133*, 13121−13129.
(35) Zeng, Z.; Murugesan, V.; Han, K. S.; Jiang, X.; Cao, Y.; Xiao, L.; Ai, X.; Yang, H.; Zhang, J.-G.; Sushko, M. L.; Liu, J. Non-Flammable Electrolytes with High Salt-to-Solvent Ratios for Li-Ion and Li-Metal Batteries. *Nature Energy* **2018**, *3*, 674−681.
(36) Wang, J. H.; Yamada, Y.; Sodeyama, K.; Chiang, C. H.; Tateyama, Y.; Yamada, A. Superconcentrated Electrolytes for a High-Voltage Lithium-Ion Battery. *Nat. Commun.* **2016**, *7*, 12032.
(37) Seo, D. M.; Reininger, S.; Kutcher, M.; Redmond, K.; Euler, W. B.; Lucht, B. L. Role of Mixed Solvation and Ion Pairing in the Solution Structure of Lithium Ion Battery Electrolytes. *J. Phys. Chem. C* **2015**, *119*, 14038−14046.
(38) Chapman, N.; Borodin, O.; Yoon, T.; Nguyen, C. C.; Lucht, B. L. Spectroscopic and Density Functional Theory Characterization of Common Lithium Salt Solvates in Carbonate Electrolytes for Lithium Batteries. *J. Phys. Chem. C* **2017**, *121*, 2135−2148.
(39) Cresce, A. V.; Russell, S. M.; Borodin, O.; Allen, J. A.; Schroeder, M. A.; Dai, M.; Peng, J.; Gobet, M. P.; Greenbaum, S. G.; Rogers, R. E.; Xu, K. Solvation Behavior of Carbonate-Based Electrolytes in Sodium Ion Batteries. *Phys. Chem. Chem. Phys.* **2017**, *19*, 574−586.
(40) Wang, F.; Borodin, O.; Ding, M. S.; Gobet, M.; Vatamanu, J.; Fan, X.; Gao, T.; Eidson, N.; Liang, Y.; Sun, W.; Greenbaum, S.; Xu, K.; Wang, C. Hybrid Aqueous/Non-aqueous Electrolyte for Safe and High-Energy Li-Ion Batteries. *Joule* **2018**, *2*, 927−937.
(41) Lin, C.-K.; Wu, I. D. Investigating the Effect of Interaction Behavior on the Ionic Conductivity of Polyester/$LiClO_4$ Blend Systems. *Polymer* **2011**, *52*, 4106−4113.
(42) Umebayashi, Y.; Mitsugi, T.; Fukuda, S.; Fujimori, T.; Fujii, K.; Kanzaki, R.; Takeuchi, M.; Ishiguro, S.-I. Lithium Ion Solvation in Room-Temperature Ionic Liquids Involving Bis-(trifluoromethanesulfonyl) Imide Anion Studied by Raman Spectroscopy and DFT Calculations. *J. Phys. Chem. B* **2007**, *111*, 13028−13032.
(43) Hardwick, L. J.; Holzapfel, M.; Wokaun, A.; Novak, P. Raman Study of Lithium Coordination in EMI-TFSI Additive Systems as Lithium-Ion Battery Ionic Liquid Electrolytes. *J. Raman Spectrosc.* **2007**, *38*, 110−112.
(44) Gafurov, M. M.; Rabadanov, K. S.; Prisyazhnyi, V. D.; Tret'yakov, D. O.; Gorobets, M. I.; Kirillov, S. A.; Ataev, M. B.; Kakagasanov, M. M. Phase Equilibriums, Ion Association, and Mechanisms of Solvation in the $LiN(CF_3SO_2)_2$-$(CH_3)_2SO_2$ System. *Russ. J. Phys. Chem. A* **2011**, *85*, 1499.
(45) Yamada, Y.; Yamada, A. Review—Superconcentrated Electrolytes for Lithium Batteries. *J. Electrochem. Soc.* **2015**, *162*, A2406−A2423.

https://dx.doi.org/10.1021/acsami.0c02706
ACS Appl. Mater. Interfaces 2020, 12, 19553−19562